Int. J. Environ. Res., 9(4):1269-1276, Autumn 2015
ISSN: 1735-6865

Preparation of Nanoporous Graphene via Nanoporous Zinc Oxide and its Application as a Nanoadsorbent for Benzene, Toluene and Xylenes Removal

Pourmand, S.[1], Abdouss, M.[1*] and Rashidi, A.M.[2]

[1]Department of Chemistry, Amirkabir University of Technology (AUT), Tehran, Iran

[2]Nanotechnology Research Center, Research Institute of Petroleum Industry (RIPI), Tehran, Iran

Received 22 Oct. 2014; Revised 31 Jan. 2015; Accepted 2 Feb. 2015

ABSTRACT: Nanoporous graphene which is used as nanosorbent was synthesized by chemical vapor deposition method via porous zinc oxide nanocatalyst. The reaction was carried out using methane as the carbon source and hydrogen as the carrier gas in a ratio of 4:1 at the temperature ranging 900-1050°C for 2-50 min. The product was characterized by scanning electron microscopy, transmission electron microscopy, thermal gravimetric analysis, Brunauer-Emmett-Teller method, x-ray diffraction, Raman and Fourier transform infrared spectroscopy. The adsorption of benzene, toluene and xylenes on to nanoporous graphene was studied. Due to the high pore volume (1.17 cm3/g), large specific surface area (410 m2/g) and small pore size, high adsorption capacity was achieved. Maximum sorption capacity of this nanosorbent for benzene, toluene and xylenes was 118.83,123.45 and 125.36 g/g nanosorbent, respectively. According to the satisfactory results achieved, nanoporous graphene can be used as a good carbon nanostructure sorbent in the removal of benzene, toluene and xylenes.

Key words: Nanoporous graphene, Adsorption, Chemical vapor deposition, Nanocatalyst

INTRODUCTION

Benzene, toluene and mixture of xylenes (BTXs) are mono aromatic hydrocarbons which are present in gasoline in 1, 1.5 and 8-10 percent volume respectively (Azev *et al.,* 2004). Relatively high water solubility of monoaromatic hydrocarbons demonstrates their great tendency to spread in contaminated waters (Lipson and Siegel 2000). According to toxicity and carcinogenic properties of these compounds, water contamination by these compounds is a very serious problem (Pohl *et al.,* 2003). BTXs have no safety threshold dose for carcinogenic effects. Thus even low-level exposure poses a finite risk (Begerow *et al.*, 1996; Sone *et al.,* 2008). Humans can be easily exposed to these compounds through skin contact, breathing and eating. Prolonged exposure causes primary and secondary harmful effects (Wolkoff and Nielsen 2001; Wallace *et al.,* 1989).These include eye and throat irritation, liver and central nervous system damage. BTXs can form photochemical smog, which contains ozone and other toxic by products, by reacting with other atmospheric chemicals such as nitrogen oxide (Das *et al.,* 2004).The presence of light aromatic hydrocarbons in water is an indicator of the presence of oil products. Major sources of monoaromatics as water contaminants are industrial wastes, leakages, spills, improper disposal and accidents during transportation of oil products. Also contamination can produced from storage tanks (that release petroleum products such as gasoline, diesel fuel, lubricating oil), gas work sites, airports, paint manufactures, chemical industries (that release pesticides, plastics, synthetic fibers) and railway yards (Vidali 2001).

It should be noticed that maximum levels of monoaromatic compounds allowed in the United States for drinking water are 0.005, 1 and 10 parts per million (ppm) for benzene, toluene and mixed xylenes, respectively (USEPA 2006).

There are several methods such as condensation, absorption, adsorption, contact oxidation and incineration that are employed for removal of organic compounds. The most commonly used process is adsorption by the adsorbents with high surface areas, pore volume, pore size distribution. The most widely utilized adsorbent for environmental cleaning is high sur-

*Corresponding author E-mail: phdabdouss44@aut.ac.ir

face area mesoporous silicates such as Mobile Crystalline Material (MCM) and Santa Barbara Amorphous type material (SBA) (Moura *et al.,* 2011).

In recent years, graphene has received considerable attention in different fields of research and has become a "star" material in recent years due to its amazing properties (John *et al.,* 1969; Lu *et al.,* 1999; Lu *et al.,* 1999; Novoselov *et al.,* 2004; Cai *et al.,* 2008; Li *et al.,* 2009; Chen *et al.,* 2011; Geim 2009; Marcano *et al.,* 2010; O'Neill *et al.,* 2011).It has been found that the nanoporous graphene has a high capacity for sorption of BTXs and other petroleum products, as well as other organic solvents, without any further modification or treatment (Bi *et al.,* 2012).

In this research, the adsorption of BTXs on nanoporous graphene was studied. The addition of sorbents to the BTXs contaminated waters facilitates a change from liquid to semi-solid phase and once this change is achieved, contaminants can be easily omitted from water by the removal of the sorbent structure. According to some unique properties of the nanoporous graphene include hydrophobicity and oleophilicity, high uptake capacity, high rate of uptake, retention over time and shaping ability, it can be used as a good candidate for the BTXs removal from water.

MATERIALS & METHODS

Nanoporous graphene was prepared by our specialchemical vapor deposition (CVD) method (Rashidi *et al.,* 2012) in a catalytic basis. The CVD technique was carried out on porous zinc oxide nanocatalyst in an electrical furnace consisting of a quartz tube with a diameter of 50 mm and 120 mm length. The furnace provided programmable heating up to 900-1050 °C for 2-50 min. The reaction was carried out using methane as the carbon source and hydrogen as the carrier gas in a ratio of 4:1.

The synthesized material was purified as follows(Arasteh *et al.,* 2010). In order to obtain pure nanoporous graphene, and remove the metal nanocatalysts, the product was stirred in 18% HCl solution for about16 h at an ambient temperature. Then the sample was washed for several times with the distilled water. The washing process continued untilthe neutral material was obtained. The treated product was dried at 100°C and characterized by SEM, TEM, TGA, BET, XRD, Raman and FT-IR spectroscopy.

Scanning electron microscopy (SEM) micrographs were taken with a CamScan MV2300 Microscope with an operating voltage of 15 kV to investigate the morphology of the samples. The nanoporous graphene was dispersed in 2-propanol and then the product was examined by transmission electron microscopy (TEM) images using a JEOL 1200 EXII microscope to verify the desired structure of the synthesized nanoporous graphene.

To evaluate the purity of nanoporous graphene, thermo-gravimetric analysis (TGA) was performed in air with a temperature ramp of 5°C/min.

Fourier transform infrared (FT-IR) spectra was recorded on a Bruker IFS 88 Fourier transform infrared Spectrophotometer with KBr pellets in the 4000-400 cm-1 region.

In addition, Raman spectroscopy, using an Almega Thermo Nicolet and 532 nm Ar-ion laser excitation source was carried out to reveal the quality of the nanoporous graphene. The main features in Raman spectra of sp2 hybridized carbon materials are the G band appearing at about 1580/cm and the 2D band at (2400-2600)/cm. In the presence of a certain amount of disorder or edges within the structure, D band appears at (1200-1400)/cm. Raman spectroscopy indicates the number of graphene layers via a change in the position and intensity of the G and 2D band (Allen et al., 2010). The surface area, pore volume and pore size distribution were measured by nitrogen adsorption at77 K using an ASAP-2010 porosimeter from the Micromeritics Corporation GA. The sample was degassed at 350 °C and 1.33-0.67 kPa overnight prior to the adsorption experiment. The pore size distribution (PSD) was evaluated from the adsorption isotherms using the Barrett, Joyner and Halenda (BJH) algorithm (ASAP-2010) available as a built-in software from Micromeritics and the standard Brunauer-Emmett-Teller (BET) method was used for the calculation of the surface area.

X-ray diffraction (XRD) patterns were recorded on Bruker D8 Advance (Cu K_radiation 0.154 nm) operating at 40 kV and 40 mA. Graphene distance layer can be calculated based on Bragg's law (James 1961; Cullity 1965):

$$n\lambda=2d_{(hkl)}\sin(\theta) \quad (1)$$

Where λ is the wavelength of the X-ray, θ is the scattering angle, n is an integer representing the order of the diffraction peak, d is the interplane distance of the lattices, and (h *kl*) are Miller indices.

The mean crystallite size of the powder composed of relatively perfect crystalline particles can be determined by Scherrer equation (James 1961; Cullity 1965):

$$L_{h\,kl} = (k\,\lambda/\beta_0\cos\theta) \quad (2)$$

where L_{hkl} is the mean dimension of the crystallite perpendicular to the plane (h *k l);* β_0 is the integral full widths at half maximum in radians; k is a constant dependent on the crystallite shape (0.89). However, the

number of graphene layers (N) can be calculated by using the following equation (Ju *et al.*, 2010):

$$N = Lh\,kl / dh\,kl \quad (3)$$

Experiments have been carried out to remove BTXs from the water samples. Physical properties of nonoporous graphene which has been used as nanosorbent are shown in Table 1. In each experiment, a specified amount of either benzene, toluene or xylenes was added to a 600-ml beaker containing 400-ml of distilled water at a constant temperature of 30°C in a water bath and stirred for a while. Immediately after the stirring stopped, one gram of nanoporous graphene was carefully weighed and added. By changing the weight ratio of the pollutants to nanosorbent, the maximum sorption capacity of the nanoporous graphene for benzene, toluene and xylenes was determined.

RESULTS & DISCUSSION

Nanoporous graphene was prepared with high pore volume. SEM image of nanoporous graphene is shown in Fig. 1(a), presents a highly porous structure with pore sizes from 45 to 63 nm. The pores provide high porosity and sufficient space for the storage of absorbed material. Likewise the capillary action which spontaneously drives the BTXs into the pores is provided by highly porous nanographene.

The TEM image of nanoporous graphene is shown in Fig.1(b).As can be observed, the structure is highly porous and the size of the graphene sheets are about 50 nm, which increase the surface area and consequently sorption capacity in comparison to the other kinds of graphene (with nonporous sheets) which are made by the other methods (Geng *et al.*, 2011; Khedr 2013; Yuan *et al.*, 2011; Jabariseresht *et al.*, 2013).

Fig. 2 shows the TGA and DTA data measured for nanoporous graphene. The weight loss of the sample in the air occurs at about 500 °C and continues to about 620°C which shows the thermal stability of the nanoporous graphene.

The functionalization process of nanoporous graphene could be also confirmed by Fourier transform infrared (FT-IR) spectroscopy, the FT-IR spectra is shown in Fig. 3(a). The peak at 3429/cm is corresponded to O-H stretching vibrations of the absorbed water molecules and structural OH groups, where peaks at 1723/cm are related to C=O stretching mode of carboxylic acid. The peak at 1628/cm is attributed to in plane C=C bound and the skeletal vibration of the graphene sheets that confirm the successful oxidation (Huh *et al.*, 2011). The peak at 1383/cm and 1123/cm is corresponded to O-H bending and C-O bending vibrations respectively.

Table 1. Physical properties deduced from N2 adsorption at 77 K on nanoporous graphene

Sample	*Bulk density* (g/cm^3)	S_{BET} (m^2/g)	S_{mi} (m^2/g)	S_{mi}/S_{BET}(%)	S_{ext} (m^2/g)	V_{mi}(cm^3/g)	V_{me} (cm^3/g)	V_{tot}(cm^3/g)	V_{mi}/V_{tot} (%)
Nanoporous graphene	0.1	410.9869	40.0398	9	370.9471	0.017844	1.173240	1.071623	1

*SBET, BET surface area; Smi, microporous surface; Sext, external surface; Vmi, micropore volume; Vme, mesopore volume; Vtot, total pore volume

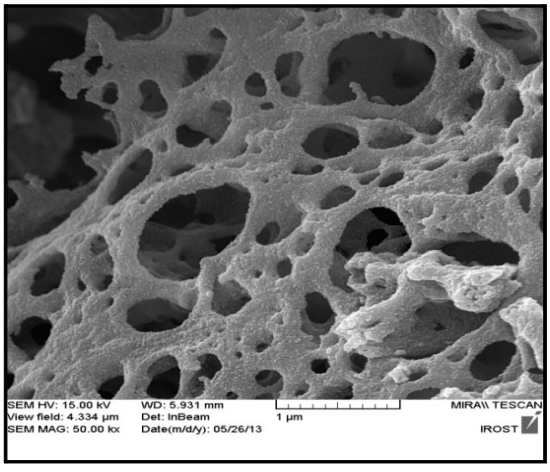

(a)

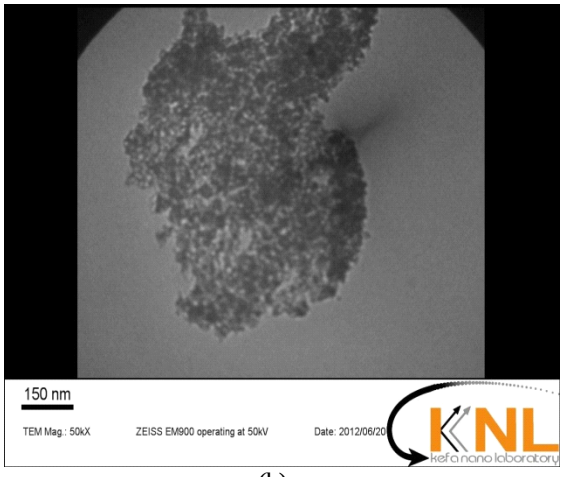

(b)

Fig. 1. (a) Scanning electron microscope image and (b) Transmission electron microscope image of nanoporous graphene

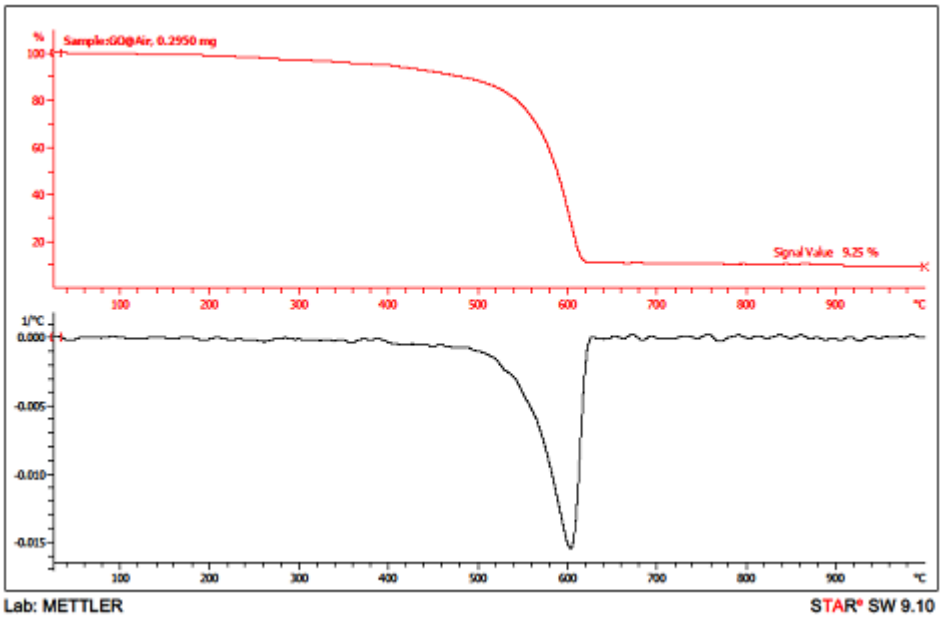

Fig. 2. TGA and DTA data of nanoporous graphene

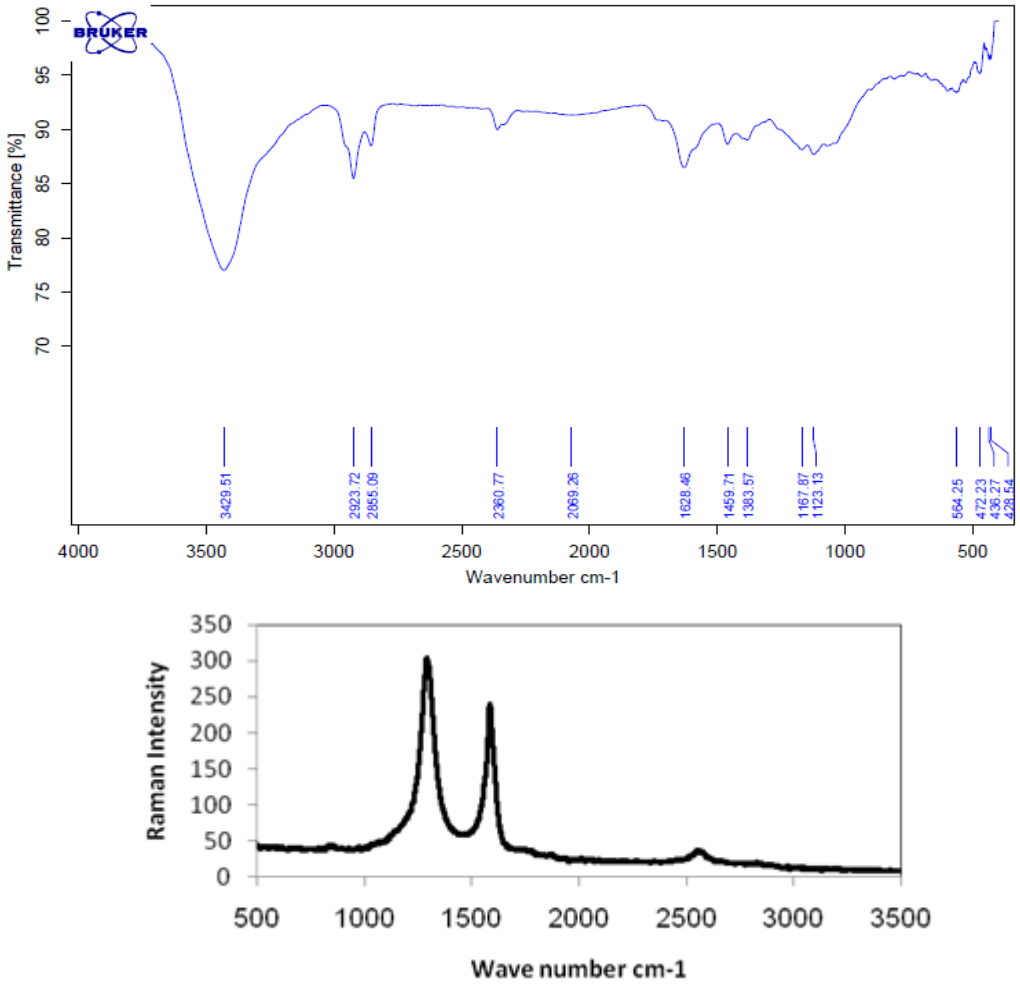

Fig. 3. (a) FT-IR and (b) Raman spectra of nanoporous graphene.

The peak at 1459/cm is corresponded to the C-C bending mode of the graphene sheets.

The Raman spectra of nanoporous graphene is shown in Fig. 3(b). The D band in 1292.5/cm is usually attributedto the presence of amorphous or disordered carbon due to the nano-sized graphitic planes and defects on these planes. The G band at 1583.5/cm is related to in-plane tangentialstretching of the carbon-carbon double bonds in the graphenesheets (Naeimi *et al.,* 2009). The intensity ratio of the D band to G band is used to evaluate the amount of disordered carbons in nanoporous graphene. The ID /IG ratio of 1.32 shows the large amount of the disordered carbons and consequently the higher adsorption capacity for the nanoporous graphene.

G band frequency of the single-layer graphene is (1585.5±1)/cm, and that of the bi-layer graphene is (1581.5±0.5)/cm.The frequency for the other thicknesses is (1582.5±1)/cm (Yoon *et al.,* 2009). The results are shown in Table 2.G band frequency is about (1582.5±1)/cm and that is why the number of nanoporous graphene layer is morethan two.

2D band at 2551/cm is also an evidence for the multilayer graphene. The 2D band can be explained by a double resonance Raman process and has a close correlation with the electronic band structure of the graphitic materials (Yoon *et al.,* 2009; Ferrari 2007). For single layer graphene, the 2D band can be seen as a sharp and symmetric peak while the 2D band shifts to higher wave numbers and becomes broader when the graphene thickness increases from single to multi layer graphene. Unfortunately, the differences in 2D band between two and a few layers of graphene sheets are not unambiguous in the Raman spectra (Ferrari 2007). According to G band frequency, broaden 2D band at 2551/cm and X-ray results, nanoporous graphene can have six layers.The N2 adsorption desorption isotherms of nanoporous graphene are shown in Fig. 4(a). The isotherms exhibit a typical type-I curve and a hysteresis loop at a relative pressure from 0.4, indicating the presence of slit shaped pores between parallel layers of nanoporous graphene (Szabo *et al.,* 2005). Physical and textural properties of nanoporous graphene were determined from N2 adsorption experiments which are presented in Table 3.

The BJH (Barrett 1951) pore size distribution is shown in Fig. 4(b). The main pore size belongs to mesoporous (2-50 nm). Mesoporous materials are an important category of nanoporous materials. Furthermore, the total pore volume of nanoporous graphene is 1.071623 cm3/g at p/p0 = 0.98. The average pore diameter, Dp, was calculated from Dp = 4VT/S (D?´az-D?´ez *et al.,* 2004), where VT is the total volume of pores, and S is been the BET surface area. Average pore diameter of 10.4 and 11.3 nm was obtained from the BET model and BJH method respectively. Average particle size was evaluated 14.6 nm. The pores with homogenous size can be seen in the range of 2-5 nm.

Fig. 5 presents the X-ray diffraction (XRD) pattern of nanoporous graphene. A peak at around 29.08°(2θ) can be seen which is the characteristic peak of graphene (Rao *et al.,* 2009), indicating that the nanoporous graphene is existed individually in single or fewer layers (Jabariseresht *et al.,* 2013).
The structural parameters such as: 2? plane (0 0 2), Interlayer distance (d) is calculated by Bargg's law(Eq. (1)), full widths at half maximum (FWHM), crystal size that is calculated by Eq. (2) and the number of graphene layers is calculated by Eq. (3) are estimated from XRD pattern and they are summarized in Table 3.

By addition of 1 g of nanoporous graphene onto the different amount of BTXs in the water, maximum sorption capacity of the nanosorbent is achieved. When the amount of BTXs in water is more than the maximum capacity of nanoporous graphene, no more compound will adsorb to the nanosorbent and the weight of the nanosorbent will no longer be increased. In Fig. 6, sorption efficiency of nanoporous graphene on benzene, toluene and xylenes is compared as histogram. Sorption capacity can be referred to as weight gain, wt%, defined as the weight of adsorbed BTXs per unit weight of the dry nanosorbent. In this case, up to 119 g benzene, 123g of toluene and 125g xylenes was adsorbed into 1 g of nanoporous graphene . Sorption rate of BTXs was so quick as to be completed within 1 min. Various kinds of graphenes and carbon nano structures have been reported with a wide range of specifications and sorption capacities for BTXs sorption (Bi *et al.,* 2012; Gui *et al.,* 2013). Among these, nanoporous graphene due to large specific surface area and high pore volume has significant advantages over other sorbent materials. Also the comparison of the maximum sorption capacity (g/g) for BTXs on different

Table 2. The G band and D band position and their intensity,intensity of D band G band ratio and 2D band position of nanoporous graphene

Sample	D band position (cm^{-1})	G band position (cm^{-1})	I_G	I_D/I_G	2D band position (cm^{-1})
Nanoporous graphene	1292.5	1583.5	192.32	1.32	2551

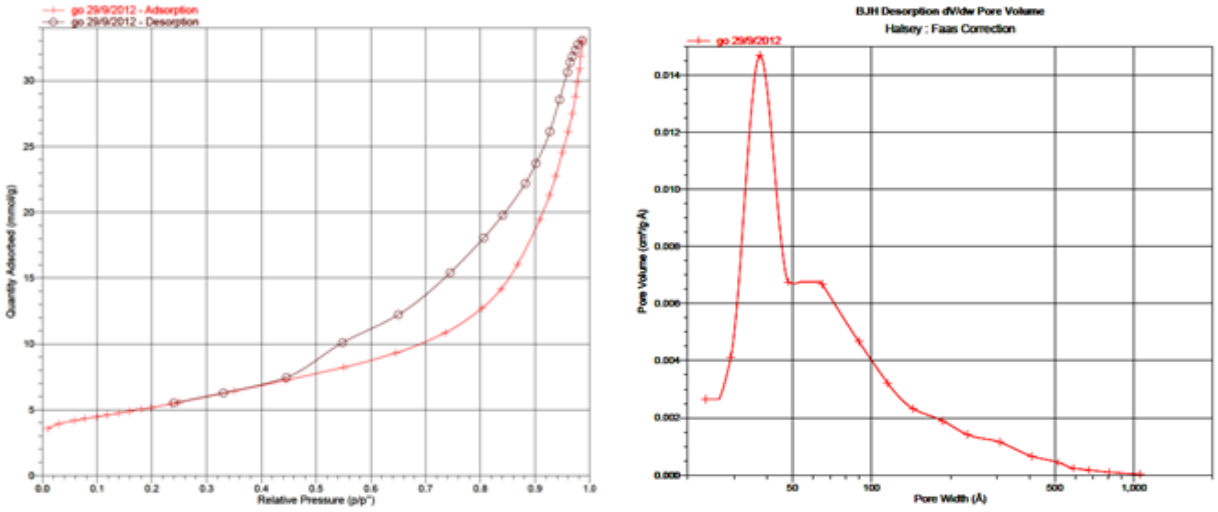

(a) **(b)**

Fig. 4. (a) Nitrogen adsorption-desorption isotherms and (b) The porosity distribution of nanoporous graphene

Table 3. X-ray structural parameters of nanoporous graphene

Sample	2θ	FWHM(°)	Layer distance(Å)	Crystal thickness (nm)	Number of layers˜
Nanoporous graphene	29.08	6.68	1.21	2.05	6

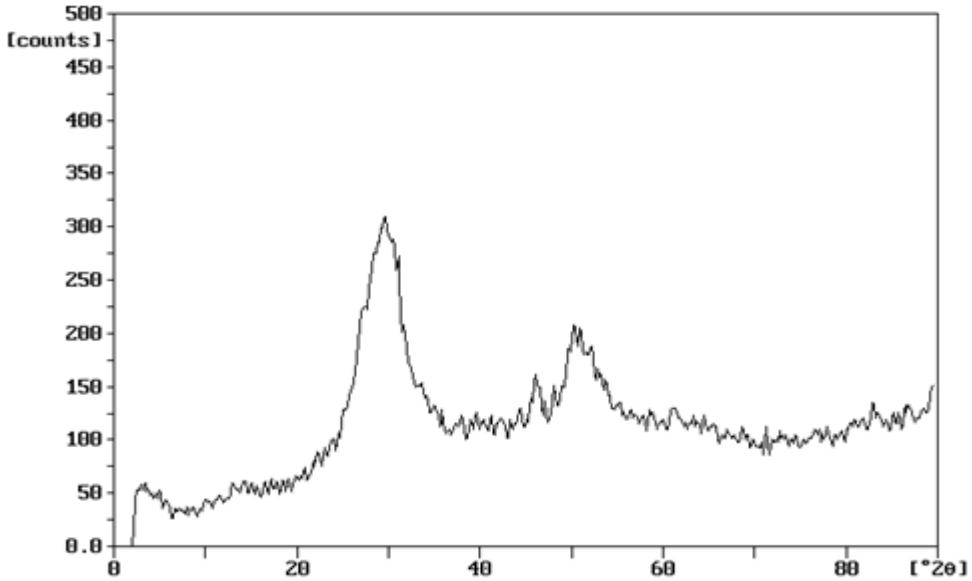

Fig. 5. X-ray diffraction pattern of nanoporous graphene

Table 4. Comparison of the maximum adsorption capacities (g/g)for BTXs by different sorbents

Sorbent	max. adsorption capacity, (g/g)			ref
	Benzene	Toluene	Xylenes	
SWCNT	0.037	0.049	0.057	Jahangiri et al., 2011
MWCNT	0.034	0.047	0.053	Jahangiri et al., 2011
Activated carbon	0.035	0.044	0.049	Jou and Tai, 1998
Carbon nanofiber	0.041	0.052	0.058	Das et al., 2004
Nanoporous carbon	0.034	0.045	0.047	Jahangiri et al., 2011
Mesoporous organo silica	0.44	0.62	0.66	Moura et al., 2011
HDTMA-modified zeolite Y	0.013	0.014	0.014	Vidal et al., 2012
Nanoporous graphene	118.8	123.4	125.4	This work

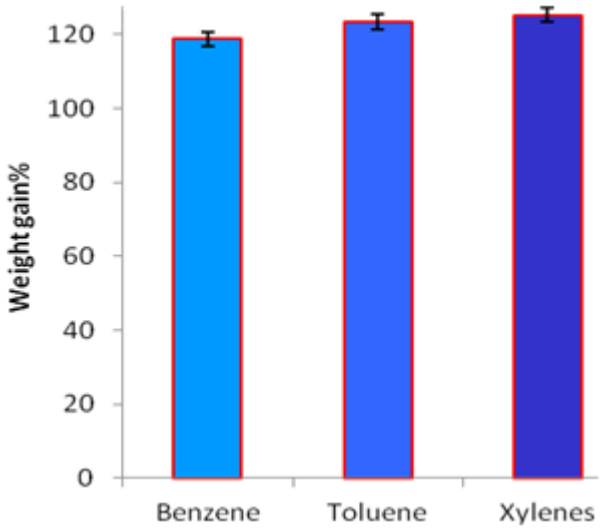

Fig. 6. Adsorption efficiency of nanoporous graphene.Weight gain is here defined as the ratio of adsorbate mass to dry weight of nanoporous graphene

sorbents is presented in Table 4. Adsorption capacity of nanoporous graphene for BTXs is greater than that for many other sorbents. It is concluded that the nanoporous graphene showed better performance than many other adsorbents in terms of adsorption capacity (Jahangiri et al., 2011; Jou and Tai 1998; Das et al., 2004; Vidal *et al.*, 2012).

CONCLUSIONS

Nanoporous graphene was prepared by special CVD method. This nanosorbent was produced with high pore volume, large specific area, small pore size and high sorption capacity. Nanoporous graphene was used as sorbent for BTXs removal from water. It showed highly sorption capacity up to 119-125g/g for BTXs.

ACKNOWLEDGEMENT

The authors gratefully acknowledge the Iran Nanotechnology Initiative Council and the Research Institute of Petroleum Industry for supporting this research.

REFERENCES

Allen, J.M., Tung, V.C.and Kaner, R.B. (2010). Honeycomb carbon: a review of graphene. Chemical Reviews, 110, 132-145.

Arasteh, R., Masoumi, M., Rashidi, A.M., Moradi, L., Samimi, V. and Mostafavi, S.T. (2010). Adsorption of 2-nitrophenol by multiwall carbon nanotubes from aqoues solutions. Applied Surface Science, **256,** 4447-4455.

Azev, V.S., Emel'yanovl, V.E. and Turovskii, F.V. (2004). Automotive gasolines long-term requirements for composition and properties. Chemistry and Technology of Fuels and Oils. **40 (5),** 291-297.

Barrett, E.P., Joyner, P.B. and Halenda, P. (1951). The determination of volume and area distribution in porous substances. I. Computations from nitrogen isotherms. Journal of the American Chemical Society, **73,** 373-380.

Begerow, J., Jermann, E., Keles, T., Koch, T. and Dunemann, L. (1996). Screening method for the determination of 28 volatile compounds in indoor and outdoor air at environmental concentrations using dual-column capillary gas chromatography with tendem electron capture-flame ionization detection. Journal of Chromatography A, **749,** 181-191.

Bi, H.C., Xie, X., Yin, K.B., Zhou, Y.L., Wan, S., He, L.B., Xu, F., Sun, L.T. and Ruoff, R. S. (2012). Spongy graphene as a highly efficient and recyclable sorbent for oils and organic solvents. Advanced Functional Materials, **22,**1-5.

Cai, W.W., Piner, R.D., Stadermann, F.J., Park, S.J., Shaibat, M.A., Ishii, Y., Yang, D.X., Velamakanni, A., An, S.J., Stoller, M., An, J., Chen, D.M. and Ruoff, R.S. (2008). Synthesis and solid-state NMR structural characterization of C-13-labeled graphite oxide. Science, **321,** 1815-1817.

Chen, S.S., Brown, L., Levendorf, M., Cai, W.W., Ju, S.Y., Edgeworth, J., Li, X.S., Magnuson, C.W., Velamakanni, A., Piner, R.D., Kang, J.Y., Park, J. and Ruoff, R.S. (2011). Oxidation resistance of graphene-coated Cu and Cu/Ni alloy. ACS Nano, **5,** 1321-1327.

Cullity, B.D. (1956). Elements of X-Ray Diffraction. (California: Addlson-Wesley Publishing Company,Inc.)

Das, D., Graur, V., Verma, N. (2004). Removal of volatile organic compounds by activated carbonfiber. Carbon, **42,** 2949.

Di´az-Di´ez, M.A., Go´mez-Serrano, V., Ferna´ndez Gonza´lez, C., Cuerda-Correa, E.M., Maci´as-Garci´a, A. (2004). Porous texture of activated carbons prepared by phosphoric acid activation of woods. Applied Surface Science, **238,** 309.

Ferrari, A.C. (2007). Raman spectroscopy of graphene and graphite: disorder, electron-phononcoupling, doping and nonadiabatic effects. Solid State Communications, **143,** 47-57.

Geim, A.K. (2009) Graphene: status and prospects. Science, **324,** 1530-1534.

Geng, D., Yang, S., Zhang, Y., Yang, J., Liu, J., Li, R., KongSham, T., Sun, X., Ye, S., Knights, S., (2011). Nitrogen doping effects on the structure of graphene. Applied Surface Science, **257,** 9193-9198.

Gui, X., Zeng, Z., Lin, Z., Gan, Q., Xiang, R., Zhu, Y., Cao, A., Tang, Z. (2013) Magnetic and highly recyclable macroporous carbon nanotubes for spilled oil sorption and separation. ACS Applied Material and Interfaces, **5,** 5845-5850.

Huh, S.H., (2011). Thermal reduction of graphene oxide,. (S. Mikhailov (Ed.) Physics and applications of graphene - experiments (pp. 73-90). Croatia: Intech.)

Jabariseresht, R., Jahanshahi, M., Rashidi, A.M. and Ghoreyshi, A.A. (2013). Synthesize and characterization of graphene nanosheets with high surface area and nanoporous structure. Applied Surface Science, **276,** 672- 681.

Jahangiri, M., Shahtaheri, S.J., Adl, J., Rashidi, A.M., Kakooei, H., RahimiForushani A., Ganjali, M.R., Ghorbanali, A. (2011). The adsorption of benzene, toluene and xylenes (BTX) onthe carbon nanostructures: the study of different parameters. Fresenius Environmental Bulletin, 20, 1036-1047.

James, R.W. (1961). X-Ray Crystallography. (New York: John Willy & Sons Inc.)

John, W. (1969). Platinum surface LEED rings, Surface Science, 17, 267-270.

Jou, C.J.G., Tai, H.S. (1998). Application of granulated activated carbon packed-bed reactor in microwave radiation field to treat BTX. Chemosphere, **37,** 685-698.

Ju, H.M., Choi, S.H., Huh, S.H. (2010). X-ray diffraction patterns of thermally-reduced graphenes, Journal of Korean Physical Society, **57,** 1649-1652.

Khedr, M.H. (2013). Preparation, decoration and characterization of graphene sheets for methyl green adsorption. Journal of Alloys and Compounds, **555,**193-200.

Lipson, D., Siegel, D.I. (2000). Using ternary diagrams to characterize transport and attenuation of BTX. Ground Water, **38 (1),** 106-113.

Li, X.S., Cai, W.W., Colombo, L. and Ruoff, R.S. (2009). Evolution of graphene growth on Ni and Cu by carbon isotope labeling. Nano Letters, **9,** 4268-4272.

Lu, X.K., Huang, H., Nemchuk, N. and Ruoff, R.S. (1999). Patterning of highly oriented pyrolytic graphite by oxygen plasma etching. Applied Physics Letters, 75, 193-195.
Lu, X.K., Yu, M.F., Huang, H. and Ruoff, R.S. (1999). Tailoring graphite with the goal of achieving single sheets. Nanotechnology, **10,** 269-272 .

Marcano, D.C., Kosynkin, D.V., Berlin, J.M., Sinitskii, A., Sun, Z., Slesarev, A., Alemany, L.B., Lu, W., Tour, J.M. (2010). Improved synthesis of graphene oxide. ACS Nano, **4,** 4806-4814.

Moura, C.P., Vidal, C.B., Barros, A.L., Costa, L.S. and Vasconcellos, L.C.G. (2011). Adsorption of BTX (benzene, toluene, o-xylene, and p-xylene) from aqueous solutions by modified periodic mesoporous organosilica. Journal of Colloid and Interface Science, **363,** 626-634.

Naeimi, H., Mohajeri, A., Moradi, L., Rashidi, A.M. (2009). Efficient and facile one pot carboxylation of multiwalled carbon nanotubes by using oxidation with ozone under mild conditions. Applied Surface Science, **256,** 631-635.

Novoselov, K.S., Geim, A.K., Morozov, S.V., Jiang, D., Zhang, Y., Dubonos, S.V., Grigorieva, I.V., Firsov, A.A. (2004). Electric field effect in automatically thin carbon films. Science, **306,** 666-669.

O'Neill, A., Khan, U., Nirmalraj, P.N., Boland, J., Coleman, J.N. (2011). Graphene dispersion and exfoliation in low boiling point solvent. Journal of Physical Chemistry, **115,** 5422-5428.

Pohl, H.R., Roney, N., Wilbur, S., Hansen, H., De Rosa, C.T. (2003). Six interaction profiles for simple mixtures. Chemosphere, **53(2),** 183-197.

Rashidi, A.M., Hajjar, Z., Ghozatllo, A., Rashtchi, M. (2012). Highly-ordered nanostructure arrays and methods of preparation thereof. US Patent 20120204890.

Rao, C.N.R., Biswas, Kanishka, Subrahmanyam, K.S., Govindaraj, A. (2009). Graphene,the new nanocarbon. Journal of Materials Chemistry, **19,** 2457-2469.

Sone, H., Fugetsu, B., Tsukada, T., Endo, M. (2008). Affinity-based elimination of aromatic VOCs by highly crystalline multi-walled carbon nanotubes. Talanta, **74,** 1265-1270.

Szabo, T., Berkesi, O., Dekany, I. (2005). DRIFT study of deuterium exchanged graphite oxide. Carbon, **43,** 3186.

USEPA (US Environmental Protection Agency), 2006. Edition of the drinking water standards and health advisories. EPA 822-R06 013, Washington, DC.

Vidal, C.B., Raulino, G.S.C., Barros, A.L., Lima, A.C.A., Ribeiro, J.P., Pires, M.J.R. and Nascimento, R.F. (2012). BTEX removal from aqueous solutions by HDTMA-modified Y zeolite. Journal of Environmental Management, **112,** 178-185.

Vidali, M. (2001). Bioremediation-an overview, Pure and Applied Chemistry, **73 (7),** 1163-1172.

Wallace, L.A., Pellizzari, E.D., Hartwell, T.D., Davids, V.,Michael, L.C., Whitmore, R.W. (1989). The influence of personal activities on exposure to volatile organic compounds. Environmental Research, **50,** 37.

Wolkoff, P., Nielsen, G.D. (2001). Organic compounds in indoor air- their relevance for perceived indoor air quality. Atmospheric Environment, **35,** 4407.

Yoon, D., Moon, H. and Che, H. (2009). Variations in the Raman spectrum as a function of the number of graphene layers. Journal of the Korean Physical Society, **55,** 1299-1303.

Yuan, W., Li, B. and Li, L. (2011). A green synthetic approach to graphene nanosheets for hydrogen adsorption. Applied Surface Science, **257,** 10183- 10187.